



Dose delivery accuracy on helical tomotherapy for 4-dimensional tumor motion — a phantom study

Raghavendra Holla¹, David Khanna², V.K. Sathiyarayanan¹

¹Ruby Hall Clinic, Pune, Maharashtra, India

²Department of Physics, Karunya Institute of Technology and Sciences, Coimbatore, India

ABSTRACT

Background: The advances in image guidance and capability of highly conformal dose deliveries made possible the use of helical tomotherapy (HT) for lung cancer treatment. To determine the effect of respiratory motion on the delivered dose in HT, film dosimetry using a dynamic phantom was performed. This was a phantom study to determine the effect of motion on the delivered dose in HT.

Materials and methods: 4D computed tomography (4DCT) was acquired for various target motions of CIRS dynamic phantom (CIRS Inc., Norfolk, USA) with 2.5cm diameter spherical target of volume 8.2 cc moving in the COS⁴ motion pattern. AvelP images and treatment plans were generated in the HT planning system. Target excursions during treatment delivery were changed in the superior-inferior, anteroposterior and lateral directions. The breathing cycle time was varied from 4 to 5 sec. and also the delivery interruptions were introduced. A film was exposed for each delivery and gamma analysis was performed.

Results: The gamma pass rate (GPR) with 3%, 2 mm criteria for the target motion in the S-I direction showed a significant reduction from 97.5% to 54.4% as the motion increased from 3 mm to 8 mm ($p = 0.03$). For the target motion in S-I = 8 mm, L-R = A-P = 3 mm, the percentage decrease in the GPR was 74% ($p = 0.001$) for three interruptions.

Conclusion: The ITV based approach in HT is ideal for a shallow breathing situation when the tumor excursions were confined to 5 mm in the S-I and 3 mm in L-R and A-P directions.

Key words: 4D CT; helical tomotherapy; dynamic phantom; target motion

Rep Pract Oncol Radiother 2021;26(3):380–388

Introduction

The treatment of inoperable lung tumors is affected by respiration and it is challenging to treat with high dose hypo-fractionated radiosurgery [1]. Radiosurgery is the preferred treatment option for non-small cell lung cancer [2]. With the advent of newer technology, there has been a rapid increase in the use of lung radiosurgery for both early-stage lung cancer and lung metastases [3]. An integrated, effective motion management

technique is necessary to treat moving targets. There are several treatment machines, such as robotic radiosurgery systems (Cyberknife, Accuray, Sunnyvale, USA) or a linac, utilizing intensity-modulated radiotherapy (IMRT) or volumetric-modulated arc therapy (VMAT) which can deliver the desired radiation dose incorporating motion management. In the absence of an integrated motion compensation technique, tumor motion has to be taken into account by adding an individual safety margin (internal margin) around the CT

Address for correspondence: Raghavendra Holla, Ruby Hall Clinic, Pune, India, 411001, tel: 8606037138; e-mail: raghavendra.holla@gmail.com

This article is available in open access under Creative Common Attribution-Non-Commercial-No Derivatives 4.0 International (CC BY-NC-ND 4.0) license, allowing to download articles and share them with others as long as they credit the authors and the publisher, but without permission to change them in any way or use them commercially

visualized clinical target volume (CTV) [4]. This can be incorporated by four-dimensional (4D) CT simulation and treatment planning to customize the margins. Maximum intensity projection (MIP) and average intensity projection (AveIP) are created from 4D CT Simulation data which is a series of three-dimensional (3D) CT image sets acquired at all the respiratory phases and sorted into different phases of the respiratory cycle. The detailed knowledge of tumour motion captured in the 4D CT is used to delineate motion encompassing target volumes, such as internal target volume (ITV) from MIP or AveIP image sets for the treatment planning [5–7]. The use of ITV for respiratory motion increases the target volume resulting in additional healthy tissue irradiation. Recently, helical tomotherapy (HT) has been explored for treating moving targets [8–11]. Gated delivery allows treatment of planning target volume (PTV) in a selected portion of the breathing waveform, between specified time intervals, or specified amplitudes, thus reducing the size of clinical and planning target volumes (CTV and PTV) by assessing the extent of target motion over one respiratory cycle. The continuous movement of the patient couch during the treatment delivery makes it difficult to implement gated delivery in HT. In the recent version of HT, such as Radixact (Accuray Incorporated, Sunnyvale, CA), real-time motion correction by tracking the moving target, without interrupting treatment delivery is compatible [12]. However, in the absence of such a modern technique, for moving tumors such as lung, the ITV based treatment is well accepted in conventional Linacs. For VMAT delivery using FF and FFF beams, ITV based treatment plans are a safe and efficient way of delivering the dose [13–15]. Various strategies, such as ITV from MIP or AveIP images, and mid position strategies (MidIP) have successfully been implemented in HT for lung tumors [8–14, 16]. But the HT treatment is delivered with continuously translating the patient couch through the gantry while the entire linear accelerator mounted on the gantry rotates around the target. Hence, the interplay between the machine dynamics and the target motion may lead to artifacts in the dose distribution [17]. Further, it has been shown that the target motion can change from day to day and even during treatment due to change in the breathing pattern making the

ITV based treatment plans inadequate for target coverage [18].

Several studies assessed the dose coverage and the target motion during HT delivery. But all these studies are limited to one-dimensional target motion [19–21]. Hence, the study was extended incorporating the target motion in all the 3 dimensions. For this, a study was designed to determine the differences in the delivered dose to the planned dose for target motion in 3 dimensions, including the superior-inferior (S-I), left-right (L-R), and anterior-posterior (A-P) directions. Further, in the current version of the HT delivery system, upon any beam interruption, the couch must be repositioned to its initial position when the beam is resumed. This will add up the chances of intra-fraction motion variability resulting in dose delivery error. Hence, a comprehensive study was performed to find the effect of treatment interruptions on the dose delivery when the target is in 3-dimensional motion.

This is a dosimetric study on a dynamic phantom was performed to determine the effect of target motion in the S-I, A-P, and L-R directions. The effect of change in the breathing cycle and the effect of treatment interruptions on the dose delivery when the target is in 3-dimensional motion was studied.

Materials and methods

Dynamic Thorax Phantom with moving target

In this study, a Dynamic Thorax Phantom model 008A (CIRS, Norfolk, VA) with CIRS motion control software (version 2.4.0) was used for treatment plan and delivery. This phantom contains a 2.5 cm diameter spherical target of volume 8.2 cc placed inside the lung volume. The CIRS phantom was set to perform a regular $\text{Cos}^{(4)}$ breathing model since the $\text{Cos}^{(4)}$ breathing model approximates the realistic patient breathing cycles with a non-constant amplitude and periodicity [19]. The target was programmed for an amplitude of 0 mm to ± 15 mm covering ± 3 , ± 5 , ± 8 , ± 10 , ± 12 , and 15mm amplitudes in the S-I direction about their corresponding reference positions with a speed of 4 seconds per cycle. In addition to the programmed S-I motion, simultaneous motions in the A-P and L-R directions were programmed from ± 0 mm, ± 3 mm, and ± 5 mm amplitudes.

A cork inserts of 6.4 cm diameter with a polystyrene film holder, which accommodates a Gafchromic EBT3 cut film of the size 6 cm × 4 cm in the sagittal plane, was indigenously designed for the plan verification. 4D CT images of the CIRS phantom with the cork inserts were acquired for all the motion dynamics as mentioned earlier and AveIP imagers were reconstructed. Delivery quality assurance plans were created using these AveIP images for all the 28 treatment plans. In these plans, the CIRS phantom was placed so that the film would pass through the PTV to ensure that the dose distribution would be measured in this region.

CT simulation and treatment planning

Cine CT images of 0.625 mm slice thickness were acquired with the tube current of 200 mA, and voltage of 120 KVp at Optima 580W CT Scanner (GE Medical Systems, Chicago, USA). 4D CT images were acquired using Smart Deviceless 4D feature from GE Medical Systems (Chicago, USA) for all the target excursions. The scan time at each table position was set to ensure that the scan covers the entire respiratory cycle per table position. Maximum Intensity Projection (MIP) and average intensity projection (AveIP) images from 10 phase binned image sets were generated using the D4D algorithm (GE Medical Systems, Chicago, USA). 36 simulations were performed for various motion combination amplitudes ranging from (0, 0, 0) to (15, 5, 5) in the [S-I, L-R, A-P] directions and CT images were acquired. The MIP and AveIP images were exported to the Precision Treatment planning system (Accuray, Sunnyvale, USA) and the ITV delineation was done

Table 1. Universal plan and optimization parameter

Delivery mode	Helical
Field width	2.51 cm
Jaw mode	Dynamic
Pitch	0.287
Modulation factor	2.000
Prescription	6.5 Gy in 1 fraction

with a consistent window width of 600 and window level of 40. An isotropic margin of 5 mm was added to ITV to generate PTV for treatment planning.

The treatment plans were generated for all the motion combination CT images as per the plan setting parameter and optimization goals in Table 1. The dose prescription was set to 6.5 Gy for 95% of the PTV.

Treatment delivery

The DQA plans were run on the tomotherapy unit with Cos⁽⁴⁾ motion for all the motion combinations in the [S-I, L-R, A-P] directions mentioned earlier. Also, the target motion ranging from 0 mm to 15 mm in S-I, 0 mm to 5 mm in A-P, and 0 mm to 5mm in the L-R direction with an increment of 3 mm was introduced during delivery. The combination of target motion in simulation and delivery are shown in the Table 2. A total of 1260 treatment deliveries (35 each for one simulated motion) covering the intended motion up to 15mm in the S-I direction and 5 mm in the A-P and L-R directions were performed. During the treatment delivery, a Gafchromic EBT3 film of 6 cm × 4 cm size was

Table 2. The target motion in S-I, L-R and A-P directions during simulation and treatment delivery

Target motion dimension in mm					
S-I direction		L-R direction		A-P direction	
Simulation	Treatment	Simulation	Treatment	Simulation	Treatment
0	0 to 15	0	0	0	0
0	0	0 to 5	0 to 5	0	0
0	0	0	0	0 to 5	0 to 5
3	0 to 15	3	0 to 5	3	0 to 5
5	0 to 15	3	0 to 5	3	0 to 5
8	0 to 15	3	0 to 5	3	0 to 5
10	0 to 15	3	0 to 5	3	0 to 5
12	0 to 15	3	0 to 5	3	0 to 5
15	0 to 15	3	0 to 5	3	0 to 5

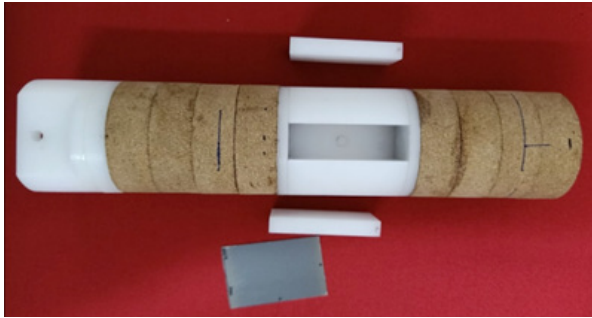


Figure 1. Sagittal plane polystyrene film holder for Gafchromic EBT3 film with the cork insert designed for Dynamic Thorax Phantom model 008A (CIRS, Norfolk, VA)

sandwiched tightly in a polystyrene film holder in the sagittal plane and placed in the cork insert as shown in Figure 1.

Delivery interruptions

For the target motion combination of [S-I, L-R, A-P], where S-I is ranging from 0 mm to 15 mm, L-R and A-P are ranging from 0 mm to 5 mm, the treatment delivery was interrupted for 1–3 times and treatment completion procedure was created and delivered. For each interruption, the patient couch was repositioned to the initial position and the partial fraction was delivered as per the completion procedure protocol of the Radixt delivery system.

Dosimetric evaluation

The exposed Gafchromic EBT3 film was scanned on Epson 10000XL Scanner after 24 hours of irradiation. Film pixel values were converted to dose using a calibration curve developed in SNC Patient software (version 8.2, Sun Nuclear Corporation, Melbourne, USA) compared to the sagittal dose map calculated by Precision treatment planning software. The dose in the film was compared with the planned dose using SNC Patient software. All the comparisons were conducted using absolute dose values. The comparison of the isodose distribution was performed by gamma analysis with the criteria of DD/DTA (i.e. DD — dose difference and DTA — distance to agreement), 3%/2 mm with 10% low dose threshold. The % of gamma pass rate (GPR) was computed with the absolute dose difference normalized to the global maximum dose and the relative DTA. In general, the 2D GPR criterion of 3%/3 has been commonly recommended for a conventional IMRT machine; hence, a stricter

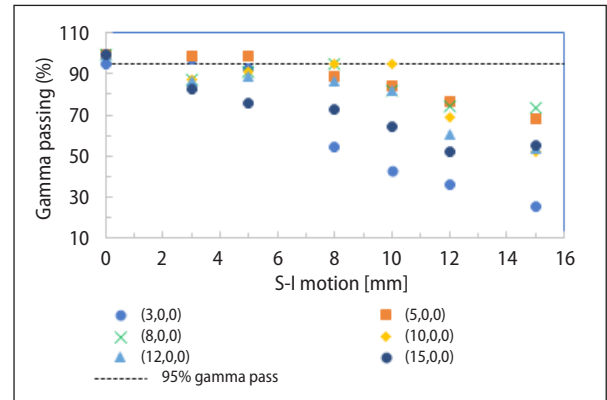


Figure 2. Gamma pass rate (GPR) for planned Vs delivery, when the target motion was in the S-I direction. The values in the parenthesis are the planned motion in the S-I, L-R, and A -P directions during the simulation. The S-I motion ranging from 0 mm to 15 mm were applied during treatment delivery

tolerance is recommended for stereotactic body radiation (SBRT) treatment [22]. Therefore, the 3%/2 mm criterion is usually used as a more restrictive GPR criterion with a 10% low dose threshold. The central-axis dose profiles along the film axis, as well as the gamma analysis results, were plotted and analyzed. The statistical analysis was performed using SPSS software ver. 21.0 (IBM, Armonk, NY, USA), and the statistical significance was set at $p < 0.05$ using student two-tailed paired t-test.

Results

Target motion in S-I direction during simulation

The GPR from the delivery sets of various target motion for S-I simulated treatment plans is shown in Figure 2. In this case, the target motion was confined to the S-I direction during the simulation. During the treatment delivery, the target motion amplitudes were varied in the S-I direction as shown in Table 2. It is found from Figure 2, that the GPR is significantly reduced as the motion in the S-I direction increases beyond 8 mm ($p = 0.03$). Further, when simultaneous motion in A -P and L-R is included, the gamma is reduced further beyond 3mm of amplitude.

Target motion in A-P direction during simulation

The GPR from the delivery sets of various target motion for A-P simulated treatment plans is shown

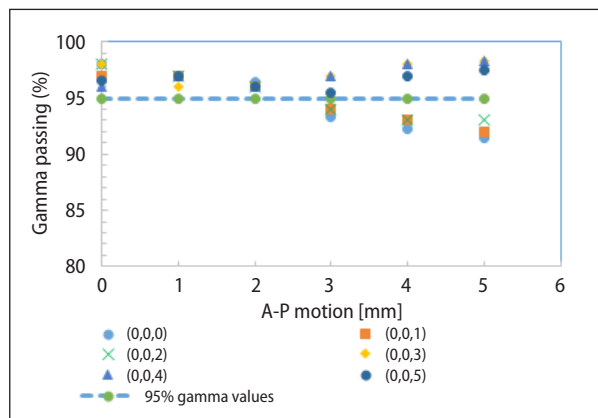


Figure 3. Gamma pass rate (GPR) for planned Vs delivery, when the target motion was in the A-P direction. The values in the parenthesis are the planned motion in the S-I, L-R, and A -P directions during the simulation. The A-P motion ranging from 0 mm to 5 mm was applied during treatment delivery

In Figure 3. In this case, the target motion was confined to the A-P direction during the simulation. During the treatment delivery, the target motion amplitudes were varied in the A-P direction as shown in Table 2. It is found from Figure 3, that the GPR was significantly reduced as the motion in the A-P direction increased beyond 3 mm during delivery for a simulated motion of 1 mm ($p = 0.02$). For a simulated A-P motion of 3 mm or more, the GPR was above 95% for the delivery motions ranging from 0 mm to 5 mm.

Target motion in L-R direction during simulation

The GPR from the delivery sets of various target motion for L-R simulated treatment plans is shown in Figure 4. In this case, the target motion was confined to the L-R direction during the simulation. During the treatment delivery, the target motion amplitudes were varied in the L-R directions as shown in Table 2. It is found from Figure 4, that the GPR is significantly reduced as the motion in the L-R direction shifts beyond 2 mm from the simulated motion ($p = 0.20$). For a treatment plan simulated with the target motion of (0, 1, 0), the delivery beyond (0, 3, 0) adding 2 mm additional motion in the L-R directions, reduces the GPR from 96% to 94%. When the L-R motion was increased to 5 mm, the GPR decreased further to 92%. For a plan of (0, 5, 0), the GPR was reduced from 97.5% to 92.5% when the motion was reduced to (0, 0, 0).

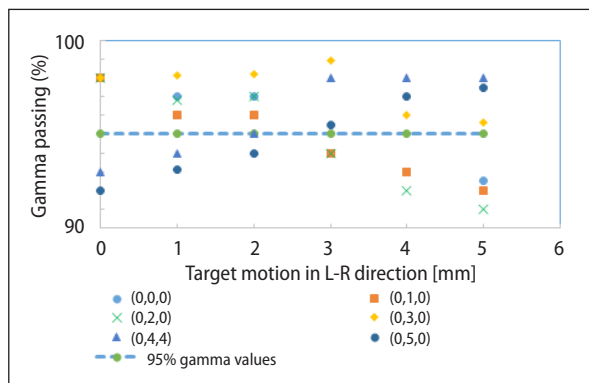


Figure 4. Gamma pass rate (GPR) for planned Vs delivery, when the target motion was in the L-R direction. The values in the parenthesis are the planned motion in the S-I, L-R, and A -P directions during the simulation. The L-R motion ranging from 0 mm to 5 mm was applied during treatment delivery

The change in the GPR was not significant when the simulated motion of 3 mm in the L-R direction increased to 5 mm during delivery ($p = 0.158$).

Simultaneous target motion in S-I, L-R, and A-P direction during simulation

The simultaneous target motion of 3,5,8, and 10 in S-I direction and 3 and 5 mm in L-R and A-P directions were applied during simulation. The treatments were delivered by varying the (S-I, L -R, A-P) dimensions from (0, 0, 0) to (15, 5, 5) mm as shown in Table 2. The GPR from the delivery sets of various target motion for simultaneous target motion simulated treatment plans are shown in Figure 5 and 6. It is found from Figure 5, that the GPR reduces below 94.5 % as the motion increases above 2 mm of the simulated motion of (3, 3, 3). For a simulated plan with the motion of (10, 3, 3), the gamma reduced to 67% when the motion was increased to (10, 5, 5) during delivery. Similarly, for a simulated target motion of (5, 5, 5), the delivery beyond (5, 3, 3) reduced the GPR below 95% ($p = 0.001$) (Fig. 6).

Effect of breathing cycles during delivery

The target motion during the simulation was kept as (3, 0, 0), (3, 3, 3), (5, 0, 0), (8, 0, 0), (8, 3, 3) and (10, 0, 0). The breathing cycle was kept at 4 seconds per cycle during the simulation. During the treatment delivery, the breathing cycle was varied to 5 secs per cycle.

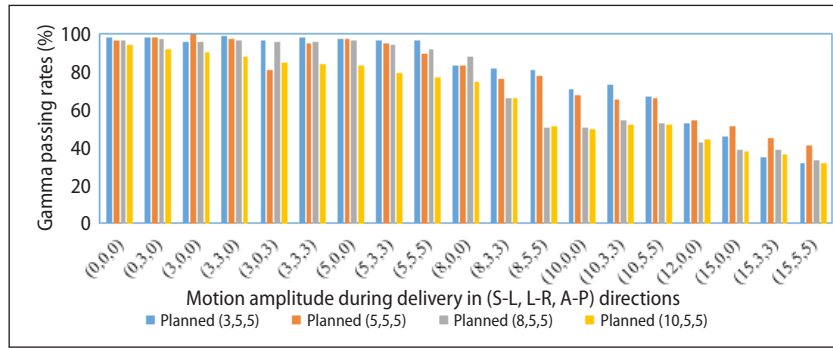


Figure 5. Gamma pass rate (GPR) for planned Vs delivery, when the target motion was in the S-I, L-R, and A-P directions. The values in the parenthesis are the planned motion in the S-I, L-R, and A-P directions during the simulation. The simultaneous motion of 3 mm on L-R and A-P was applied with the S-I motion ranging from 0 mm to 10 mm during the simulation. During the treatment delivery, simultaneous motion ranging from 0 mm 5 mm in the L-R and A-P directions with the S-I motion ranging from 0 mm to 15 mm were applied

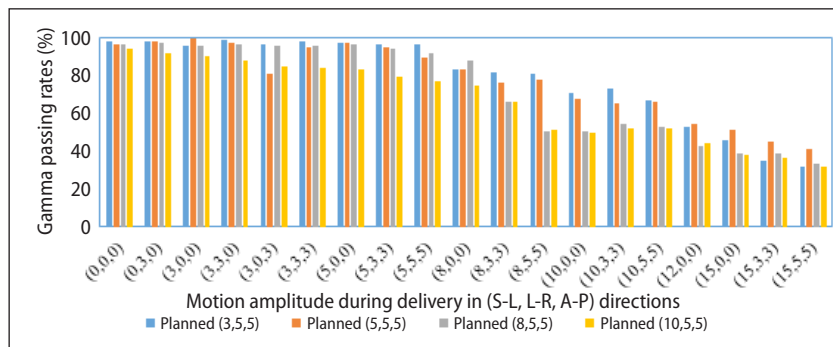


Figure 6. Gamma pass rate (GPR) for planned Vs delivery, when the target motion was in the S-I, L-R, and A-P direction. The values in the parenthesis are the planned motion in the S-I, L-R, and A-P directions during the simulation. The simultaneous motion of 5 mm on L-R and A-P was applied with the S-I motion ranging from 0 mm to 10 mm during the simulation. During the treatment delivery, simultaneous motion ranging from 0 mm 5 mm in the L-R and A-P direction with the S-I motion ranging from 0 mm to 15 mm was applied

The breathing cycle time did not influence the GPR up to the target motion of (5, 0, 0). When the target motion was increased to 8 mm in the S-I direction, the GPR was decreased from 95.1% to 82.5 % ($p = 0.006$) for 4-sec to 5-sec breathing cycle (Fig. 7).

Delivery interruptions

In this case, the delivery was interrupted up to 3 times during the treatment. The original delivery without interruption was compared with the one, two, and three interruptions. From Figure 8, the interruptions did not influence the GPR up to the 5 mm motion in the S-I direction. When the S-I motion was increased to 5 mm, with the A-P and L-R motion of 3 mm applied simultaneously, the GPR decreased from 95% to 74% ($p = 0.001$) for 3 interruptions.

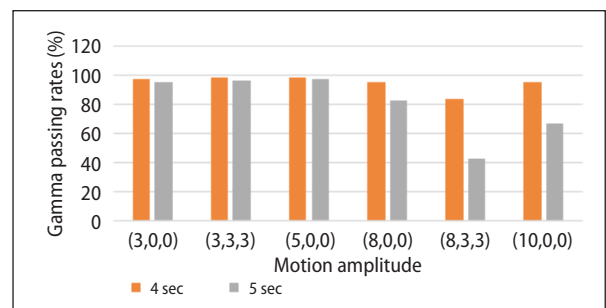


Figure 7. Gamma pass rate (GPR) in % for planned Vs delivery for 4 and 5 sec breathing cycle time

Discussions

The present work focused on the delivery accuracy in tomotherapy in the presence of target motion in the S-I, L-R, and A-P directions. In this

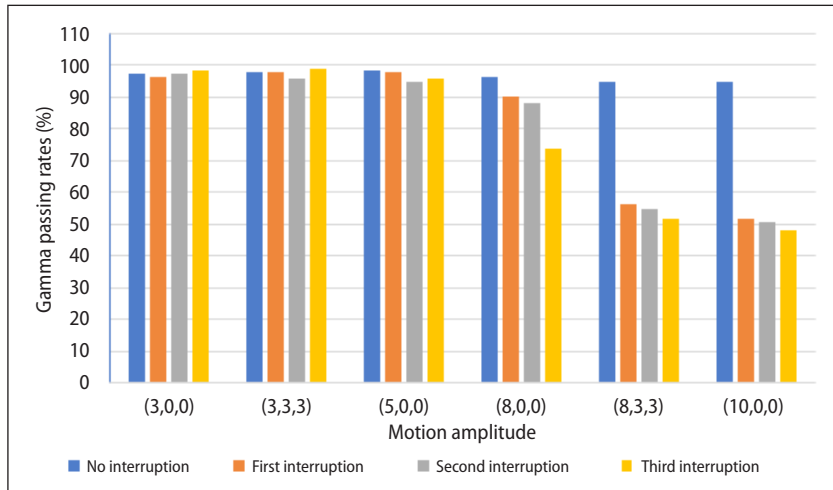


Figure 8. Gamma pass rate (GPR) in % for planned Vs delivery for 0, 1, 2, and 3 interruptions during treatment delivery

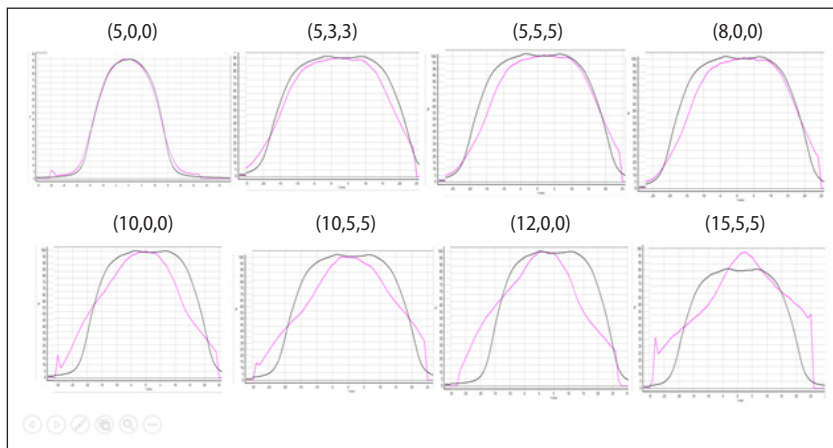


Figure 9. The dose profile comparison between the planned (black) and delivered dose (magenta) on a moving phantom on the central axis of the target in the longitudinal axis. The values in the parenthesis are the target motion during the delivery in (S-I, L-R, A-P) direction for a planned target excursion of (5, 0, 0)

study, the treatment accuracy by gamma analysis was studied using a film when the target is subjected to various motion during simulation and treatment. It was necessary to study the treatment accuracy during helical delivery of the treatment and apply an appropriate strategy for the moving targets in tomotherapy delivery. This study assumed that there would be a good correlation between the simulation and treatment delivery for moving targets. Also, this correlation would be consistent over the entire course of the treatment when the treatment was delivered for different tumor motion, breathing cycle, and treatment interruptions. This was achieved with the help of the CIRS dynamic phantom with target motion in known dimensions. The gamma passing systematically showed lower

values for the moving target when the target motion was increased by more than 3 mm in the S-I and 3 mm in A-P and L-R directions. This could be due to the limitation of the helical delivery as the tumor motion takes a larger amplitude, and the chances of missing the intended target dose due to the phase mismatch between couch positions in the Z-direction and the gantry rotation with the target motion as shown in the Figure 9.

The difference in the GPR with the planned dose increased for longer breathing cycle time. The difference was significant for the combination of motion above (8, 0, 0) in (S-I, L -R, A-P) directions. As the cycle time increased, for a target motion up to 5 mm in the S-I direction, the increase in the breathing cycle from 4 sec to 5 sec did not change

the GPR. This is mainly due to the averaging effect of the delivered dose since the target trajectory is small. But when the target motion was increased to 8 mm in the S-I direction, the delivered dose was less than the intended dose. This was evident in the GPR.

The treatment interruptions did not influence the delivery accuracy as long as the target motion was within (5, 0, 0). When the target motion was increased to (5, 3, 3), the GPR decreased significantly from 96.5% to 74% for zero interruption to 3 interruptions. This decrease is not due to the HT machine capability to pick up the treatment from the interruption since for a static tumor, the interruptions did not decrease the GPR during the commissioning of the machine for clinical use. This mismatch could be due to the result of a synchronization mismatch between couch translation to the target motion. This difference increased as the motion in the S-I direction increased as shown in Figure 8.

These observations show that even after generating a proper ITV from AveIP images using 4D CT, the dose coverage to the target is suboptimal when the target moves differently than simulation. The GPRs were in the acceptable limit when the target motion was up to 5 mm in the S-I direction with the A-P and L-R motion up to 3 mm. This was the case even for the simultaneous motion of the target.

In lung SBRT, the irradiation time has the highest influence on the dose coverage. The irradiation time in HT strongly depends on the planning parameters used for the treatment plan preparation such as modulation factor, pitch, which is the ratio of couch translation per rotation to the field width, and field width. Decreasing the modulation factor reduces treatment time with reduced plan quality. Hence, the modulation factor of 2.0 was fixed at all the treatment plans in this study. Further, small pitch value introduces leaf time inaccuracies with smaller leaf opening times (LOT) [23]. The treatment time was reduced by almost 50% when the field width (FW) changed from 2.5 cm to 5 cm but at the cost of less optimal dose distribution. And also, for a tumor of the size 2.5 cm diameter, the use of 5 cm field width is sub-optimal since motion excursions used in this study for the target in the S-I direction was only up to a maximum of 15 mm. The pitch of 0.287 and modulation factor of

2.0 were chosen so that the gantry period is maintained at 15 seconds to improve treatment accuracy by increasing the LOT and, thereby, reducing the delivery time.

Conclusion

In a phantom study, when high target motion is involved, the ITV based approach is ideal for a shallow breathing situation where the tumor excursions were confined to 5 mm in the S-I direction and 3 mm in the L-R and A-P directions.

If the tumor motion is above 5 mm in the S-I direction, a change in the breathing cycle by 1 sec, introduced significant error in the delivered dose. The influence of delivery interruptions during the treatment delivery for a moving target showed a significant reduction in the GPR for target excursions of above 5 mm in the S-I and 3 mm in L-R and A-P directions when the delivery interruption was more than one.

Conflict of interest

None declared.

Funding

None declared.

Data sharing statement

All data generated and analyzed during this study are included in this published article.

References

1. Adamczyk M, Konkol M, Matecka-Nowak M, et al. 4DCT-based evaluation of lung tumour motion during the breathing cycle. *Neoplasma*. 2020; 67(1): 193–202, doi: [10.4149/neo_2019_190309N206](https://doi.org/10.4149/neo_2019_190309N206), indexed in Pubmed: [31847524](https://pubmed.ncbi.nlm.nih.gov/31847524/).
2. Guckenberger M, Krieger T, Richter A, et al. Potential of image-guidance, gating and real-time tracking to improve accuracy in pulmonary stereotactic body radiotherapy. *Radiother Oncol*. 2009; 91(3): 288–295, doi: [10.1016/j.radonc.2008.08.010](https://doi.org/10.1016/j.radonc.2008.08.010), indexed in Pubmed: [18835650](https://pubmed.ncbi.nlm.nih.gov/18835650/).
3. Franks KN, Jain P, Snee MP. Stereotactic ablative body radiotherapy for lung cancer. *Clin Oncol (R Coll Radiol)*. 2015; 27(5): 280–289, doi: [10.1016/j.clon.2015.01.006](https://doi.org/10.1016/j.clon.2015.01.006), indexed in Pubmed: [25746732](https://pubmed.ncbi.nlm.nih.gov/25746732/).
4. Landberg T, Chavaudra J, Dobbs J, et al. Report 62. *Journal of the International Commission on Radiation Units and Measurements*. 2016; os32(1), doi: [10.1093/jicru/os32.1.report62](https://doi.org/10.1093/jicru/os32.1.report62).
5. Kruis MF, van de Kamer JB, Belderbos JSA, et al. 4D CT amplitude binning for the generation of a time-averaged

- 3D mid-position CT scan. *Phys Med Biol.* 2014; 59(18): 5517–5529, doi: [10.1088/0031-9155/59/18/5517](https://doi.org/10.1088/0031-9155/59/18/5517), indexed in Pubmed: [25170633](https://pubmed.ncbi.nlm.nih.gov/25170633/).
6. Giraud P, Garcia R. [Respiratory gating for radiotherapy: main technical aspects and clinical benefits]. *Bull Cancer.* 2010; 97(7): 847–856, doi: [10.1684/bdc.2010.1143](https://doi.org/10.1684/bdc.2010.1143), indexed in Pubmed: [20605765](https://pubmed.ncbi.nlm.nih.gov/20605765/).
 7. Seppenwoolde Y, Shirato H, Kitamura K, et al. Precise and real-time measurement of 3D tumor motion in lung due to breathing and heartbeat, measured during radiotherapy. *Int J Radiat Oncol Biol Phys.* 2002; 53(4): 822–834, doi: [10.1016/s0360-3016\(02\)02803-1](https://doi.org/10.1016/s0360-3016(02)02803-1), indexed in Pubmed: [12095547](https://pubmed.ncbi.nlm.nih.gov/12095547/).
 8. Boggs D, Feigenberg S, Walter R, et al. Stereotactic radiotherapy using tomotherapy for early-stage non-small cell lung carcinoma: Analysis of intrafraction tumour motion. *J Med Imaging Radiat Oncol.* 2014; 58(6): 706–713, doi: [10.1111/1754-9485.12179](https://doi.org/10.1111/1754-9485.12179), indexed in Pubmed: [24767098](https://pubmed.ncbi.nlm.nih.gov/24767098/).
 9. Gallo JJ, Kaufman I, Powell R, et al. Single-fraction spine SBRT end-to-end testing on TomoTherapy, Vero, TrueBeam, and CyberKnife treatment platforms using a novel anthropomorphic phantom. *J Appl Clin Med Phys.* 2015; 16(1): 5120, doi: [10.1120/jacmp.v16i1.5120](https://doi.org/10.1120/jacmp.v16i1.5120), indexed in Pubmed: [25679169](https://pubmed.ncbi.nlm.nih.gov/25679169/).
 10. Hodge W, Tomé WA, Jaradat HA, et al. Feasibility report of image guided stereotactic body radiotherapy (IG-SBRT) with tomotherapy for early stage medically inoperable lung cancer using extreme hypofractionation. *Acta Oncol.* 2006; 45(7): 890–896, doi: [10.1080/02841860600907329](https://doi.org/10.1080/02841860600907329), indexed in Pubmed: [16982555](https://pubmed.ncbi.nlm.nih.gov/16982555/).
 11. Nagai A, Shibamoto Y, Yoshida M, et al. Safety and efficacy of intensity-modulated stereotactic body radiotherapy using helical tomotherapy for lung cancer and lung metastasis. *Biomed Res Int.* 2014; 2014: 473173, doi: [10.1155/2014/473173](https://doi.org/10.1155/2014/473173), indexed in Pubmed: [24995299](https://pubmed.ncbi.nlm.nih.gov/24995299/).
 12. Schnarr E, Beneke M, Casey D, et al. Feasibility of real-time motion management with helical tomotherapy. *Med Phys.* 2018; 45(4): 1329–1337, doi: [10.1002/mp.12791](https://doi.org/10.1002/mp.12791), indexed in Pubmed: [29405307](https://pubmed.ncbi.nlm.nih.gov/29405307/).
 13. Wanet M, Sterpin E, Janssens G, et al. Validation of the mid-position strategy for lung tumors in helical TomoTherapy. *Radiother Oncol.* 2014; 110(3): 529–537, doi: [10.1016/j.radonc.2013.10.025](https://doi.org/10.1016/j.radonc.2013.10.025), indexed in Pubmed: [24424385](https://pubmed.ncbi.nlm.nih.gov/24424385/).
 14. Adamczyk M, Kruszyna-Mochalska M, Rucińska A, et al. Software simulation of tumour motion dose effects during flattened and unflattened ITV-based VMAT lung SBRT. *Rep Pract Oncol Radiother.* 2020; 25(4): 684–691, doi: [10.1016/j.rpor.2020.06.003](https://doi.org/10.1016/j.rpor.2020.06.003), indexed in Pubmed: [32581656](https://pubmed.ncbi.nlm.nih.gov/32581656/).
 15. Sterpin E, Janssens G, Orban de Xivry J, et al. Helical tomotherapy for SIB and hypo-fractionated treatments in lung carcinomas: a 4D Monte Carlo treatment planning study. *Radiother Oncol.* 2012; 104(2): 173–180, doi: [10.1016/j.radonc.2012.06.005](https://doi.org/10.1016/j.radonc.2012.06.005), indexed in Pubmed: [22841518](https://pubmed.ncbi.nlm.nih.gov/22841518/).
 16. Kim B, Chen J, Kron T, et al. Motion-induced dose artifacts in helical tomotherapy. *Phys Med Biol.* 2009; 54(19): 5707–5734, doi: [10.1088/0031-9155/54/19/004](https://doi.org/10.1088/0031-9155/54/19/004), indexed in Pubmed: [19729710](https://pubmed.ncbi.nlm.nih.gov/19729710/).
 17. Minn AY, Schellenberg D, Maxim P, et al. Pancreatic tumor motion on a single planning 4D-CT does not correlate with intrafraction tumor motion during treatment. *Am J Clin Oncol.* 2009; 32(4): 364–368, doi: [10.1097/COC.0b013e31818da9e0](https://doi.org/10.1097/COC.0b013e31818da9e0), indexed in Pubmed: [19398901](https://pubmed.ncbi.nlm.nih.gov/19398901/).
 18. Zhu Z, Fu X. The radiation techniques of tomotherapy & intensity-modulated radiation therapy applied to lung cancer. *Transl Lung Cancer Res.* 2015; 4(3): 265–274, doi: [10.3978/j.issn.2218-6751.2015.01.07](https://doi.org/10.3978/j.issn.2218-6751.2015.01.07), indexed in Pubmed: [26207214](https://pubmed.ncbi.nlm.nih.gov/26207214/).
 19. Kanagaki B, Read PW, Molloy JA, et al. A motion phantom study on helical tomotherapy: the dosimetric impacts of delivery technique and motion. *Phys Med Biol.* 2007; 52(1): 243–255, doi: [10.1088/0031-9155/52/1/016](https://doi.org/10.1088/0031-9155/52/1/016), indexed in Pubmed: [17183139](https://pubmed.ncbi.nlm.nih.gov/17183139/).
 20. Hu Y, Archibald-Heeren B, Byrne M, et al. Investigating the impact of tumour motion on TomoTherapy stereotactic ablative body radiotherapy (SABR) deliveries on 3-dimensional and 4-dimensional computed tomography. *Australas Phys Eng Sci Med.* 2019; 42(1): 169–179, doi: [10.1007/s13246-019-00727-8](https://doi.org/10.1007/s13246-019-00727-8), indexed in Pubmed: [30790140](https://pubmed.ncbi.nlm.nih.gov/30790140/).
 21. Dunn L, Kron T, Taylor ML, et al. A phantom for testing of 4D-CT for radiotherapy of small lesions. *Med Phys.* 2012; 39(9): 5372–5383, doi: [10.1118/1.4742053](https://doi.org/10.1118/1.4742053), indexed in Pubmed: [22957605](https://pubmed.ncbi.nlm.nih.gov/22957605/).
 22. Klein EE, Hanley J, Bayouth J, et al. Task Group 142, American Association of Physicists in Medicine. Task Group 142 report: quality assurance of medical accelerators. *Med Phys.* 2009; 36(9): 4197–4212, doi: [10.1118/1.3190392](https://doi.org/10.1118/1.3190392), indexed in Pubmed: [19810494](https://pubmed.ncbi.nlm.nih.gov/19810494/).
 23. Westerly DC, Soisson E, Chen Q, et al. Treatment planning to improve delivery accuracy and patient throughput in helical tomotherapy. *Int J Radiat Oncol Biol Phys.* 2009; 74(4): 1290–1297, doi: [10.1016/j.ijrobp.2009.02.004](https://doi.org/10.1016/j.ijrobp.2009.02.004), indexed in Pubmed: [19394157](https://pubmed.ncbi.nlm.nih.gov/19394157/).